INT. J. REMOTE SENSING, 1994, VOL. 15, NO. 3, 711-718

Fire and glint in AVHRR's channel 3: a possible reason for the non-saturation mystery

A. W. SETZER

INPE-C.P. 515-12201, São José dos Campos, SP, Brazil, and
Institute for Remote Sensing Applications, Joint Research Centre,
TP 440, I-21020 Ispra (VA), Italy

and M. M. VERSTRAETE

Institute for Remote Sensing Applications, Joint Research Centre,
TP 440, I-21020 Ispra (VA), Italy

(Received 9 July 1993; in final form 1 October 1993)

Abstract. Evidence from a very strong and rare case of sunglint in a NOAA-11 AVHRR image is used to show that a problem exists in the on-board signal processing of channel 3. This problem, associated only with targets of high reflectivity and/or temperature, causes erroneous indication of digital counts (DN) and calculated brightness temperatures for near-saturation ranges in channel 3 images. The explanation proposed, a spurious conversion of the sensor signal to DNs, fits observations of sunglint and fire detection data in AVHRR images of the NOAA-series satellites which could not otherwise be explained.

1. Introduction

Channel 3 (3·55-3·93 μm) of the Advanced Very High Resolution Radiometer (AVHRR) on-board the NOAA-series satellites is sensitive to emitted as well as reflected energy in the optical spectrum. It supposedly saturates for Earth targets at about 47° C, or 320K (Kidwell 1991), and also with light from sunglint in water bodies (Khattak *et al.* 1991) or sun light reflected from some types of exposed soils (Grégoire *et al.* 1993). Snow, ice, and ice clouds, however, reflect relatively little in the channel 3 spectral region; most other clouds also reflect less than sunglint (Scorer 1989). According to Wien's displacement law, the thermal emission of vegetation fires in the range 400-700° C peaks in the 3-4 μm range and calculations predict (e.g., Matson and Dozier 1981; Robinson 1991) that a fire of about 30 m × 30 m in extent and near the centre of a channel 3 pixel should saturate it. This expectation is not supported by available measurements, however. For instance, large fires in forests and grasslands, sometimes occupying areas many times the size of an AVHRR pixel (1·1 × 1·1 km at nadir) have been associated repeatedly with non-saturated values of channel 3 (Belward *et al.* 1993, Pereira and Setzer 1993, Setzer and Malingreau 1993a, Setzer *et al.* 1993). For sunglint no actual data are apparently found in the literaure. Brush (1993) showed an NOAA-12 AVHRR scene where the signal 'may' reach saturation; he also pointed to a 'transient' effect just entering the sunglint area, which will be easily explained with the new finding presented below. This transient signal, which appears in the channel 3 images like an atmospheric halo/corona effect around the sunglint area, whatever its size, as well as the non-saturation by very large fires may be the result of the on-board signal processing problem we believe to have found. This letter presents the evidence for our hypothesis.

2. Case description and discussion

Figure 1 shows the NOAA-11 AVHRR image used, where Indo-China is on the west side and the Philippines on the east. Its contrast has been enhanced artifically just for illustration purposes and the data analysis was performed using the raw uncorrected data with full 1·1 km (nominal) and 10-but maximum resolutions. The sunglint area in the South China Sea is shown in red. This image was recorded during orbit number 07698, with an ascending equatorial crossing of approximately 06:03 hours GMT and 121° W, and downloaded at Wallops Island, VA, USA. The sunglint in the image occurred at a scan angle of about 23°. Such specular reflection is commonly observed when the Sun is near the AVHRR's scanning plane. Uncommon in the image is the small sunglint region in the north Borneo coastline. Figure 2 shows an enlargement of the relevant area, in the centre of Brunei Bay, at 5° N and 115° W. The unusual characteristic of this small spot of sunglint is its

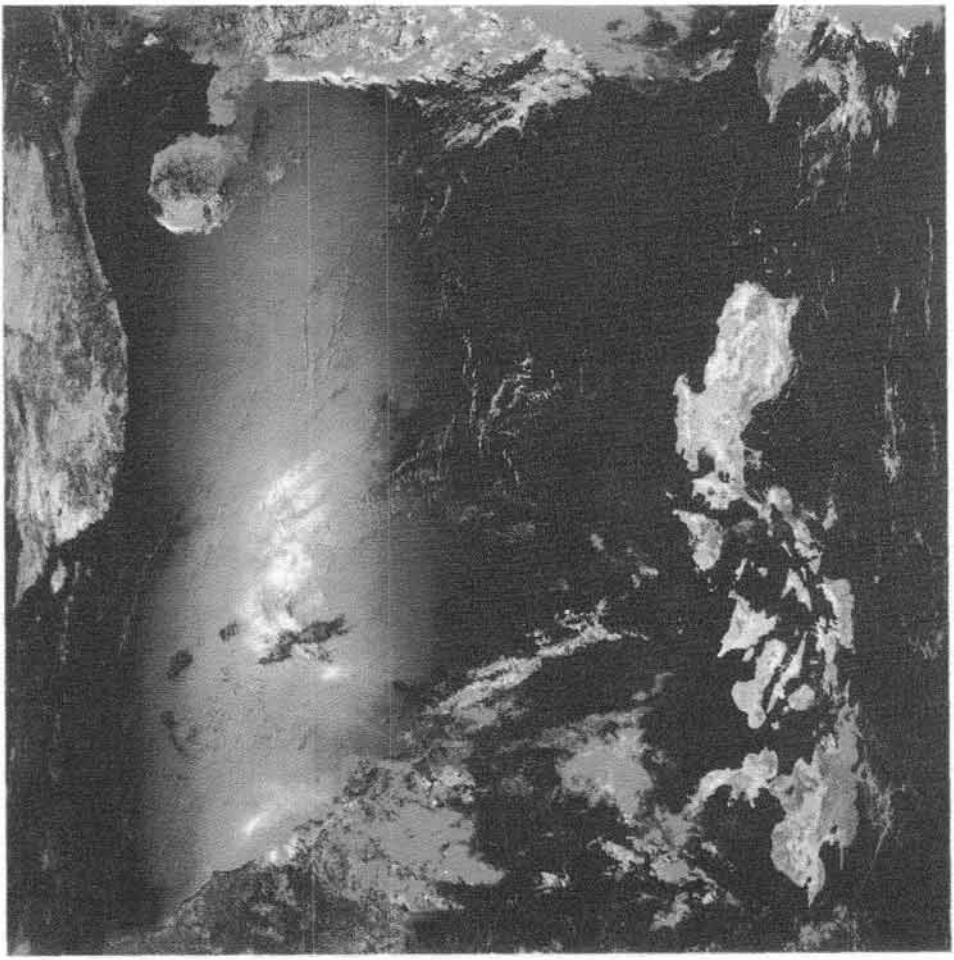

Figure 1. Raw AVHRR false-colour composite image showing sunglint in the South China Sea. Indo-China and the Gulf of Tonkin with Hai-Nan island are seen in the upper left corner; the Philippines are in the right side and Borneo in the lower side.

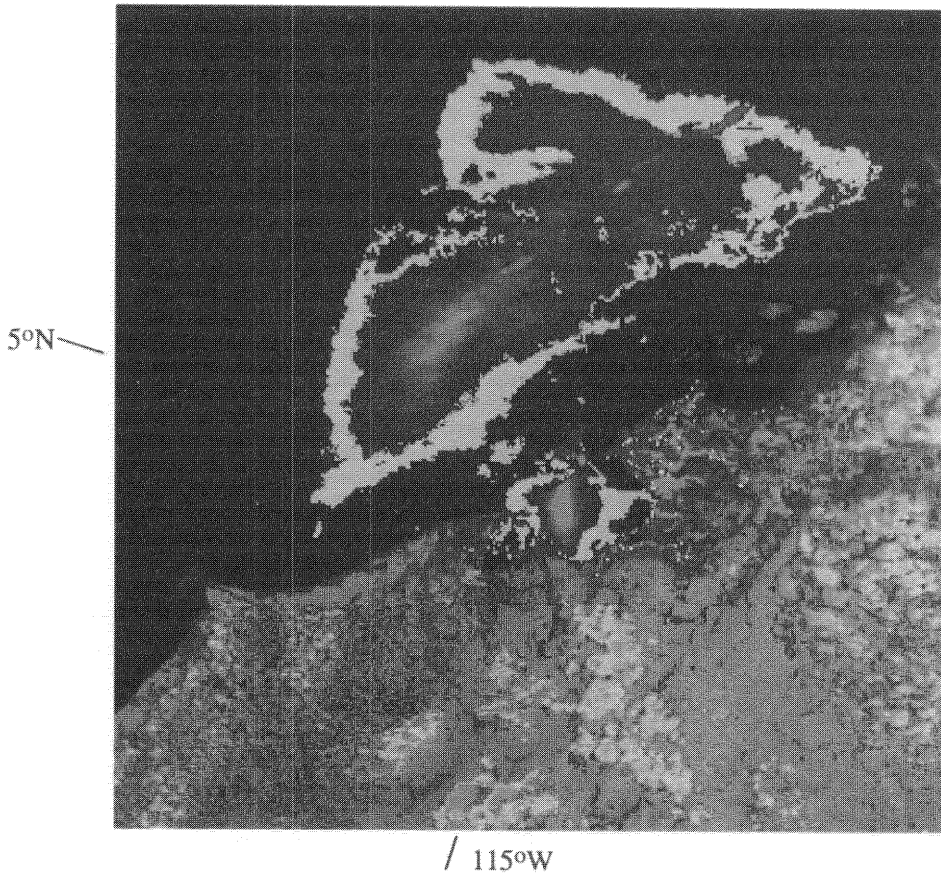

Figure 2. Very strong sunglint in the Brunei Bay at 5° N and 115° W, in the north coast of Borneo. Note 'halo' effect in red colour surrounding also the larger and less intensive sunglint further north.

intensity, which can be analyzed from figure 3. This figure shows the digital counts (DN) of individual raw pixels in the original 0–1023 (10-bit) scale, for channels 1 to 4, for an area of 15×15 pixels with the sunglint at its centre. A saturated pixel with DN 1023 is found in channel 1 (0·55–0·68 μm)—see figure 3(*a*), and another with DN 1001, i.e., close to saturation, is found in channel 2 (0·75–1·1 μm)—see figure 3(*b*). In these two channels most pixels at the core of the sunglint, in the shaded area, have DNs above 700 and this is what makes the case unusual: normally, sunglint is associated with DNs in the 200–400 range, only rarely reaching the 600's or higher. Unquestionably, this is a case of 'metallic reflection from a water surface', using Scorer's (1989) terminology. The explanation for such high reflectance is likely to be the absence of waves (Khattak *et al.* 1991) in the wind protected waters of a closed bay.

An extreme case of sunglint such as this one should have saturated channel 3 also, but this is not observed. Channel 3 DNs in figure 3(*c*) are shown in their natural inverted scale, where saturation corresponds to 0 and very low temperature/reflectivity to 1023. We observe that the core of the sunglint is represented by pixels

Channel 01

y \ x	577	578	579	580	581	582	583	584	585	586	587	588	589	590	591
2945	229	233	240	243	249	263	312	402	501	490	386	331	297	284	270
2946	236	238	246	254	268	304	375	497	653	554	404	337	308	289	271
2947	245	246	255	267	292	331	421	701	836	540	395	339	308	284	272
2948	253	259	268	287	309	347	576	1023	918	577	419	357	309	283	269
2949	259	268	281	302	331	449	908	972	830	608	447	359	310	285	270
2950	258	273	295	319	368	644	982	912	623	511	437	376	322	290	276
2951	262	279	296	319	380	696	973	983	794	502	410	361	325	296	280
2952	266	277	296	326	411	775	996	953	932	562	419	351	313	293	279
2953	261	281	307	355	458	717	1003	1013	910	614	443	366	322	297	284
2954	263	277	295	331	390	587	842	917	878	700	486	393	337	305	288
2955	256	262	279	302	359	491	671	795	832	735	512	393	342	310	288
2956	246	259	277	304	356	460	606	738	749	648	504	398	342	314	292
2957	241	258	276	305	345	417	527	629	666	622	520	415	358	324	294
2958	240	261	284	307	327	355	458	590	625	601	508	412	352	315	289
2959	245	265	288	299	313	337	392	493	621	639	514	400	339	312	291

Channel 02

y \ x	577	578	579	580	581	582	583	584	585	586	587	588	589	590	591
2945	196	201	206	210	215	227	271	349	434	421	333	285	256	243	232
2946	203	204	212	219	232	264	328	435	566	477	347	290	264	248	232
2947	211	212	220	231	253	290	370	612	717	464	340	291	264	244	233
2948	219	224	232	249	269	306	508	895	796	493	358	306	265	242	230
2949	223	232	243	264	290	397	797	974	721	525	384	308	266	243	231
2950	222	236	256	278	325	572	963	789	536	440	375	322	275	247	236
2951	226	241	258	278	337	620	979	951	676	430	352	310	279	253	240
2952	230	240	258	284	365	686	953	1001	800	478	357	300	268	250	238
2953	225	242	266	309	402	636	880	925	783	522	377	312	275	253	242
2954	223	236	253	285	340	517	736	802	759	597	414	336	288	260	245
2955	216	221	236	259	310	428	586	689	719	630	436	335	292	264	244
2956	208	218	234	258	305	397	526	641	648	557	430	338	291	268	248
2957	201	216	232	258	294	358	454	544	574	533	442	352	305	276	249
2958	196	215	236	258	276	304	395	509	539	516	434	351	299	268	245
2959	197	212	233	248	264	286	337	427	537	548	438	341	290	267	248

Channel 03

y \ x	577	578	579	580	581	582	583	584	585	586	587	588	589	590	591
2945	22	25	30	33	36	38	42	43	43	43	43	42	41	40	39
2946	28	29	34	37	39	42	43	43	44	43	43	42	42	41	39
2947	35	35	37	39	41	42	43	44	44	43	43	42	42	41	40
2948	37	38	39	41	42	43	43	45	45	43	43	43	42	40	39
2949	38	39	40	42	42	43	45	45	44	43	43	43	42	41	39
2950	37	40	41	42	43	44	45	45	43	43	43	43	42	41	40
2951	38	40	41	42	43	44	45	45	44	43	43	43	42	41	40
2952	39	40	41	42	43	44	45	45	44	43	43	42	42	41	40
2953	38	40	42	43	43	44	45	45	44	43	43	43	42	41	40
2954	38	40	41	42	43	43	44	45	45	44	43	43	42	42	41
2955	36	37	40	41	43	43	44	44	44	44	43	43	42	42	41
2956	32	36	40	41	42	43	43	44	44	44	43	43	42	42	41
2957	28	36	39	41	42	43	43	43	43	44	43	43	43	42	41
2958	21	35	40	41	42	43	43	43	44	43	43	43	42	42	41
2959	26	35	40	41	42	42	43	43	43	44	43	43	42	42	41

Channel 04

y \ x	577	578	579	580	581	582	583	584	585	586	587	588	589	590	591
2945	385	385	383	382	382	382	381	380	379	379	379	379	379	380	381
2946	383	383	381	380	381	380	378	378	378	378	379	379	380	381	382
2947	381	381	380	380	379	378	377	378	378	379	380	380	381	381	381
2948	380	380	380	379	377	376	376	377	379	380	381	381	381	381	380
2949	380	380	379	378	377	375	376	378	380	380	380	380	380	380	380
2950	379	379	378	377	377	376	377	379	380	379	379	380	380	379	380
2951	379	378	378	378	378	378	378	379	380	380	381	381	381	380	381
2952	379	379	379	379	379	378	379	379	379	380	381	382	382	381	381
2953	378	378	377	377	376	376	376	377	378	379	380	381	381	381	381
2954	377	376	374	375	376	376	376	376	376	377	378	378	379	379	380
2955	378	377	376	377	378	378	377	378	378	378	378	378	378	379	380
2956	379	378	378	378	378	378	378	379	380	379	379	379	378	379	379
2957	380	379	379	378	378	378	378	379	381	381	381	379	379	379	379
2958	379	379	378	378	378	377	378	380	381	382	382	380	379	379	379
2959	376	376	376	377	378	378	377	379	381	383	382	381	380	379	378

Figure 3. AVHRR digital counts (DNs) for pixels in the centre of intense sunglint. See table 1 for the limits of classes used for channels 1 to 3.

with a DN 45 instead of the expected value of zero. We further observe from figure 3 that the signal in channel 3 is positively correlated to the signals of channels 1 and 2. Therefore, surprisingly, the reflectance/temperature signal in channel 3 increases (lower DNs on the inverted scale) outwards from the sunglint while the reflectance decreases in the visible and near IR channels. The DN ranges for channels 1 and 2, associated with DN values of 45–41 in channel 3 for the data subset shown in figure 3, are listed in table 1. DNs of channels 1 and 2 for the corresponding channel 3 DNs of 46 to 49 found outside the intense sunglint inverted this trend and were in the following ranges, respectively: 195 to 200, and 168 to 170.

Figure 4 shows the profiles of pixel values for all 5 channels for a segment of an AVHRR scan line (2952 in figure 3) passing through the core of the sunglint. The peaks of channels 1 and 2 coincide and indicate unambiguously the core of the sunglint where they reach values at or close to saturation. Channels 4 and 5, on the other hand are not sensitive to reflected sun light and show no noticeable variation in the core of the sunglint area. This implies that the sea surface temperature must have been essentially constant throughout the area. Using calibration coefficients provided with the data, the nominal temperature for the area of figure 3 was close to 23° C and the variation was only a few tenths of one degree C. The interesting finding is that the curve for channel 3 reaches saturation at two other places, away from the core of the sunglint, at totally unexpected places.

This finding could however be explained by a faulty on-board conversion of the analogue signal from the channel 3 sensor into DNs. This conversion should in principle take place monotonically, i.e., associate progressively lower DNs to increasing radiance measurements. Instead, we postulate that beyond a specific threshold radiance, increasing radiances are transformed into increasing DNs. In this type of curve, schematically shown in figure 5, a signal level higher than the level corresponding to a null DN results in DNs previously allocated to lower signal levels. Therefore, in figure 4 we believe that the correct curve for channel 3 should be a kind of mirror image with respect to the x axis for those pixels situated in the interval between the pixels where saturation is first reached.

The areas with a DN of zero are shown with a red tone in figure 2 and can be found surrounding the sunglint regions following the pattern of the graph in figure 4. In addition to the Brunei Bay, another and larger sunglint to the north can be seen in the same figure, but presenting DNs in channels 1 and 2 in the common ranges below 400. This edge effect with pixels of zero DN, which gives the impression of a corona/halo/transient effect, is easily explained as resulting from a signal conversion curve like the one in figure 5. We also want to emphasize that this edge effect of

Table 1. Class ranges in the core of the intense sunglint.

Channel 3	Channel 12	Channel 2
45	>878	>759
44	622–877	533–758
43	347–621	304–532
42	302–346	260–303
41	285–301	243–259
40	272–284	233–242

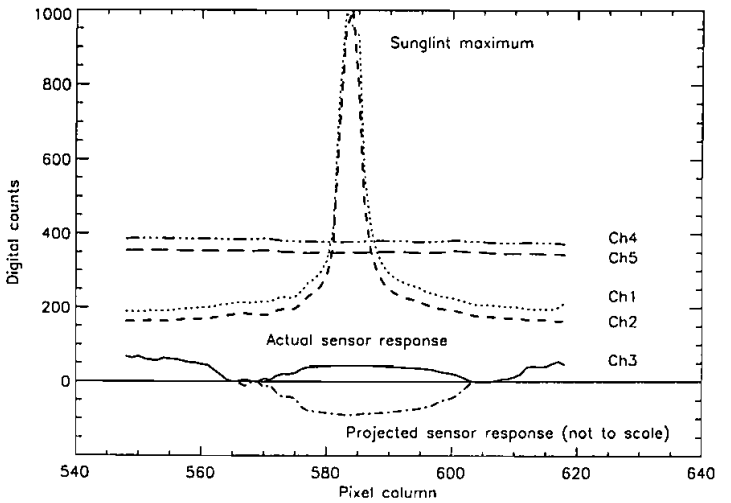

Figure 4. Line transect through an intense sunglint in an AVHRR image. Actual pixel values for the central part are found in figure 3, line 2952.

channel 3 was found not only in the two cases shown in figure 2, but also in all other cases of sunglint in dozens of NOAA-11 AVHRR channel 3 images we have examined.

This interpretation of anomalous data can be confirmed independently by analyzing data from an entirely different process, namely fire detection over continents in AVHRR channel 3 images. Vegetation fires, no matter their temperature or size, provided the fire front is larger than ~50 m, do not saturate channel 3 (Belward *et al.* 1993, Pereira and Setzer 1993, Setzer and Malingreau 1993a, Setzer *et al.* 1993), contrary to calculations based on the emitted energy (e.g.,

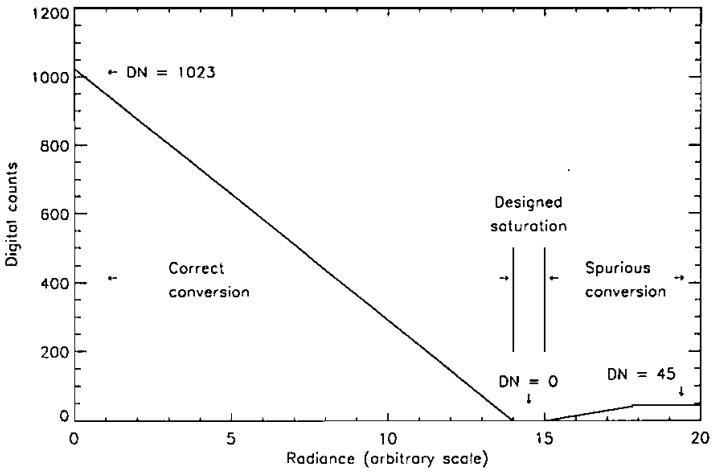

Figure 5. Hypothetical channel 3 conversion of radiance into digital counts.

Matson and Dozier 1981; Robinson 1991). Furthermore, actively burning fires were consistently associated with a DN of 45 in channel 3 during March, 1990 (Setzer and Malingreau 1993 a, b, precisely the same value found in the core of our exceptional sunglint. When examining histograms of channel 3 images containing many fires or sunglint a very steep change in their profiles was regularly found at DN 45 indicating a discontinuity at this point. We conclude that our postulated engineering problem would also explain why hot fires over continents do not saturate channel 3 pixels. This could further imply that AVHRR channel 3 may actually be observing much higher temperatures than currently estimated on the basis of existing data, calibration coefficients and established calibration procedures given by Kidwell (1991). Finally, the fact that at least NOAA-9 AVHRR exhibited the same pattern of non-saturation of channel 3 over active fires (Pereira and Setzer 1993, Setzer and Pereira 1991) suggests that the same problem may affect multiple AVHRR instruments; histogram discontinuities for fire pixels in NOAA-9 AVHRR similar to what we found for NOAA-11 AVHRR can be seen in Brustet *et al.* (1991) and Pereira and Setzer (1993).

3. Conclusion

Our observation of particular DN values associated with targets which should, but do not saturate AVHRR's channel 3 is corroborated with analyses of a large number of AVHRR scenes both over oceans (sunglint) and continents (sunglint and fires). Our claim concerning a possible design flaw in the instrument circuitry could be confirmed by a thorough evaluation of the instrument. As far as channel 3 users are concerned, estimates of fire temperatures and sunglint energy becomes now a valid exercise combining a proposition along the pattern of figure 5 with the multispectral information of AVHRR from existing fire and sunglint data—an attractive possibility to extend the channel 3 range to 500° C or more. Unfortunately, highly reflective exposed soils in some cases will also have the same DN signal as fires in the defective AVHRR images, precluding a general application of AVHRR's image in fire monitoring. As for the future AVHRRs, if our hypothesis is correct, two possibilities exist: either leave the sensor in its current condition and alert users of the problem, or make the 0–1023 digital range match the sensor output. A third option, the elimination of the signal after the currently designed saturation limit of ~47° C, would limit even more its use in such an important application as fire detection.

Acknowledgment

We acknowledge the support of the Brazilian Scientific Council (CNPq) which made the development of this work possible through grant no. 200602/79-9.

References

BELWARD, A. S., GRÉGOIRE, J. M., D'SOUZA, G., TRIGG, S., HAWKES, M., BRUSTET, J. M., SERCA, D., TIREFORD, J. L., CHARLOT, J. M., and VUATTOUX, R., 1993. *In-situ*, real time fire detection using NOAA/AVHRR data. *6th European AVHRR Data Users' Meeting, Belgirate, Italy, 28 June–2 July, Italy, Proceedings*, CEC/JRC, Ispra, Italy, in press.

BRUSH, R. J. H., 1993. Anomalous effect of sunglint on the AVHRR in the NOAA-12 satellite. *International Journal of Remote Sensing*, **14**, 629–634.

BRUSTET, J. M., VICKOS, J. B., FONTAN, J., MANISSADJAN, K., PODAIRE, A., and LAVENU, F., 1993. Remote sensing of biomass burning in West Africa with NOAA-AVHRR. In

Global Biomass Burning, edited by J. S. Levine (Cambridge, Mass.: The MIT Press), pp. 47–52.

GRÉGOIRE, J. M., BELWARD, A. S., and KENNEDY, P., 1993. Dynamiques de saturation du signal dans la bande 3 du senseur AVHRR: handicap majeur ou source d'information pour la surveillance de l'environnement en milieu soudano-guinéen d'Afrique de l'Ouest? *International Journal of Remote Sensing*, **14**, 2079–2095.

KHATTAK, R. A., VAUGHAN, R. A., and CRACKNELL, A. P., 1991. Sunglint and its observation in AVHRR data. *Remote Sensing of Environment*, **37**, 101–116.

KIDWELL, K. B., 1991. NOAA polar orbiter data user's guide. NOAA/NESDIS, Washington, D.C.

MATSON, M., and DOZIER, J., 1981, Identification of subresolution high temperature sources using thermal IR sensor. *Photogrammetric Engineering and Remote Sensing*, **47**, 1311–1318.

PEREIRA, M. C., and SETZER, A. W., 1993, Spectral characteristics of deforestation fires in NOAA/AVHRR images. *International Journal of Remote Sensing*, **14**, 583–597.

ROBINSON, J. M., 1991. Fire from space: Global fire evaluation using infrared remote sensing. *International Journal of Remote Sensing*, **12**, 3–24.

SCORER, R. S., 1989, Cloud reflectance variations in channel-3. *International Journal of Remote Sensing*, **10**, 675–686.

SETZER, A. W., and MALINGREAU, J. P., 1993 a. Temporal variation in the detection limit of fires in AVHRR's ch. 3. *6th European AVHRR Data Users' Meeting, Belgirate, Italy, 28 June–2 July, Italy, 6 pp.* CEC/JRC, Ispra, Italy, in press.

SETZER, A. W., and MALINGREAU, J. P., 1993 b. AVHRR monitoring of vegetation fires in the tropics: towards a global product. Submitted to *Remote Sensing of Environment*.

SETZER, A. W., and PEREIRA, M. C., 1991, Amazonia biomass burning in 1987 and an estimate of their tropospheric emissions. *Ambio*, **20**, 19–22.

SETZER, A. W., PEREIRA, M. C., and PEREIRA JR., A. C., 1993, Satellite studies of biomass burning in Amazonia—some practical aspects. *Remote Sensing Reviews*, in press.